Supplementary Information for

Enhancing photosensitivity via assembly of a uranyl coordination polymer

Miaomiao Xu,[‡,a,c] Huangjie Lu,[‡,c] Chunhui Wang,[b] Jie Qiu,[,b] Zhaofa Zheng,[c] Zhi-Hui Zhang,[a] Xiaofeng Guo,[d] Ming-Yang He,[a] Junfeng Qian,[a,*] and Jian Lin[b,*]*

[a] Jiangsu Key Laboratory of Advanced Catalytic Materials and Technology, Changzhou University, Changzhou 213164, China

[b] School of Nuclear Science and Technology, Xi'an Jiaotong University, No.28, West Xianning Road, Xi'an, 710049, P. R. China

[c] Shanghai Institute of Applied Physics, Chinese Academy of Sciences, 2019 Jia Luo Road, Shanghai 201800, P. R. China

[d] Department of Chemistry and Alexandra Navrotsky Institute for Experimental Thermodynamics, Washington State University, Pullman, Washington 99164- 4630, United States;

‡ These authors contributed equally to this work.

Table of Content

S1. Experimental section.

Caution! *Depleted uranium was used in this study. Standard protection for radioactive materials should be followed in an authorized laboratory designed for actinide element studies.*

Reagents. $UO_2(NO_3)_2 \cdot 6H_2O$ (99.9%), 2,6-di(1H-pyrazol-1-yl)isonicotinic acid (98%, Jilin Chinese Academy of Sciences-Yanshen Technology Co., Ltd), DMF (99.5%, Aladdin), and CH_3COOH (99.5%, Sinopharm Chemistry Reagent Co., Ltd) were used as received from commercial suppliers without further purification.

Synthesis: $UO_2(NO_3)_2 \cdot 6H_2O$ (5.02 mg, 0.01 mmol), 2,6-bis(pyrazol-1-yl)pyridine carboxylic acid (2.56 mg, 0.01 mmol), DMF (100 μL), and deionized water (400 μL) were loaded into a 5 mL glass vial and heated in an oven at 100 °C for 72 h. After cooling to room temperature, yellow acicular crystals of **U-bppCOO** were isolated. The crystals were washed with ethanol and dried under ambient conditions.

S2. Characterizations.

X-ray crystallography. Single crystal X-ray diffraction measurements were performed using a Bruker D8-Venture single crystal X-ray diffractometer equipped with an IμS 3.0 microfocus X-ray source (Mo–Kα radiation, λ = 0.71073Å) and a CMOS detector at 298 K. The data frames were collected using the program *APEX3* and processed using the program *SAINT* routine in *APEX3*.[1] The structures were solved by the direct method and refined on F^2 by full-matrix least-squares methods using *SHELXTL* program.[2] During the refinement of **U-bppCOO**, a large residual electron density was located in the difference Fourier map with a short distance of 0.465 Å to U1, suggesting disorder of U1. The disorder was modeled with two sites and constrained to a single-site sum, giving rise to an occupancy of 0.555/0.445. U(1) is coordinated by seven O atoms, which are disordered as well. Modeling of the disorder O atoms over two sites the same occupancy of 0.555/0.445 gave reasonable displacement parameters and U−O bond distances (Table S2).

Powder X-ray diffraction (PXRD) data were collected from 5 to 50° with a step of 0.02° and the time for data collection was 0.15 s on a Bruker D8 Advance diffractometer with Cu Kα radiation (λ = 1.54056 Å) and a Lynxeye one-dimensional detector.

UV-Vis Absorption and luminescence Spectroscopy. The UV-Vis absorption and luminescence spectra of **U-bppCOO** and bppCOOH were recorded on a Craic Technologies microspectrophotometer. Crystals of **U-bppCOO** or powder sample of bppCOOH were placed on a quartz slide and data was collected after auto-set optimization. During the collection of luminescence spectra, an optical filter masking signal below 420 nm was applied to eliminate the interference of excitation light. The UV radiation was provided by a 365 nm UV lamb (0.82 kW/m^2) and the X-ray radiation was provided by an X-ray tube with tungsten filament (60 kV, 12 W, and 7.2 kGy/h).

Electron Spin-Resonance (ESR) spectroscopy. The electron spin-resonance spectroscopy for nonirradiated and irradiated samples was recorded in JEOL-FA200 spectrometer. An X-band spectrometer (JES-FA200) with 100-kHz field modulation was interfaced with a computer to manipulate the spectra. The integrate spectral intensity ESR measurements were performed at room temperature and the microwave power used was 1.0 mW.

Thermogravimetric Analysis (TGA). TGA was carried out in an N_2 atmosphere with a heating rate of 10 ℃/min from 30 ℃ to 900 ℃ on a NETZSCH STA 449 F3 Jupiter instrument.

Detection Limit Calculation. The calibration curves were established by plotting the quenching rate $(I_0 - I)/I_0$ (%) as a function of dose. Since **U-bppCOO** features an emission maximum centering at 518 nm, the luminescence intensities at 518 nm were chosen to calculate the LOD toward UV dose. The curves at the low dose range were fitted with linear correlations. The LODs were calculated using the following equations:

$$\text{LOD} = 3\sigma/\text{slope}$$

$$\sigma = 100\times(I_{SE}/I_0)$$

where I_{SE} is the standard error of the fluorescence intensity measurement, as determined by the baseline measurement of blank samples.

S3. Supplementary Figures.

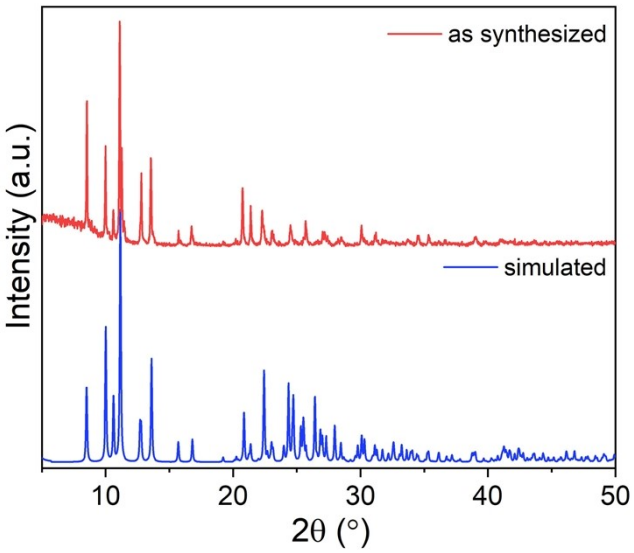

Fig. S1 PXRD pattern of as-synthesized **U-bppCOO** compared with the simulated one.

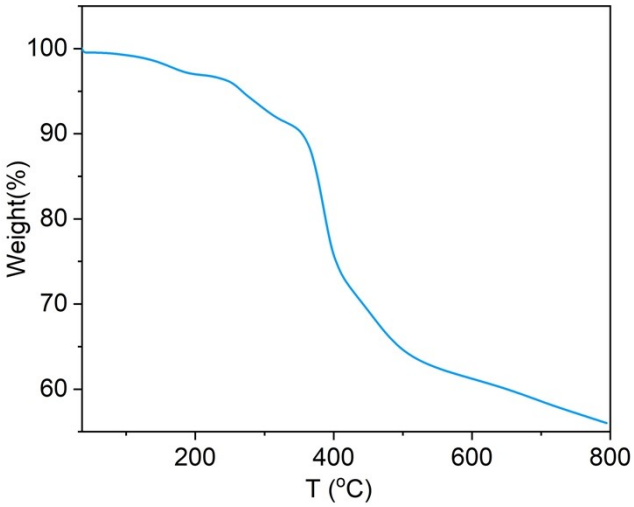

Fig. S2 Thermogravimetric curve of **U-bppCOO**.

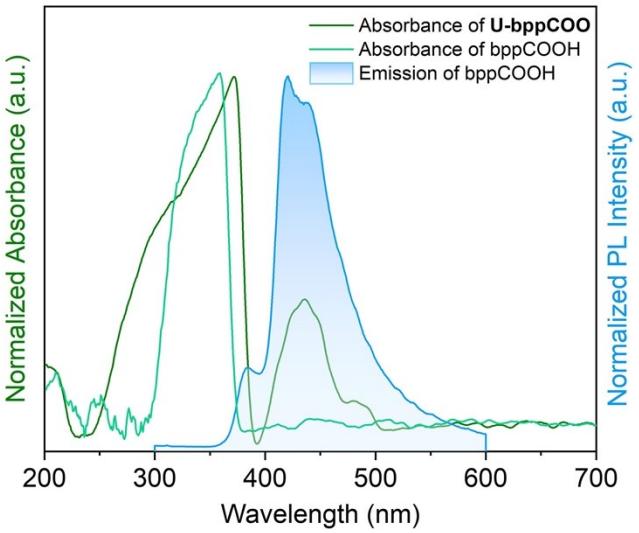

Fig. S3 The UV-Vis absorption spectra of **U-bppCOO** and bppCOOH, and the luminescence spectrum of bppCOOH ligand.

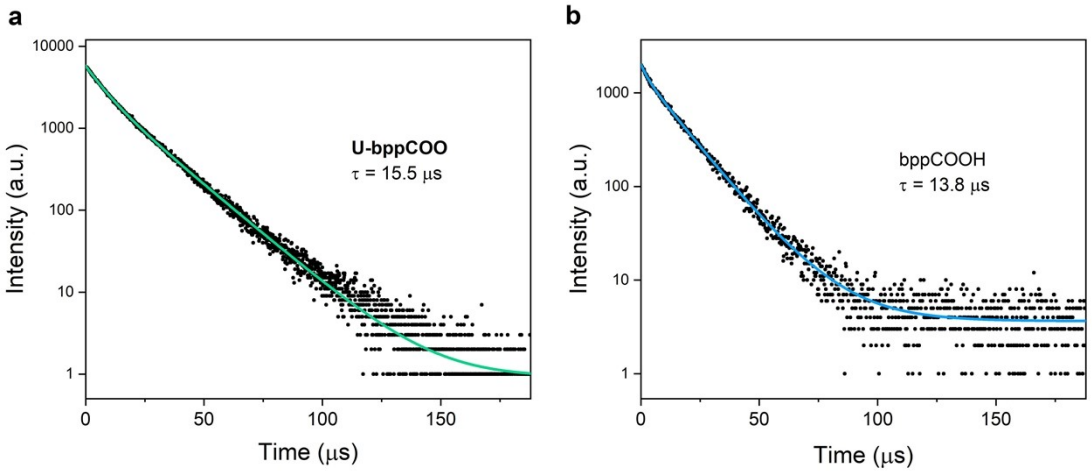

Fig. S4 Photoluminescence lifetimes of (a) **U-bppCOO** and (b) bppCOOH.

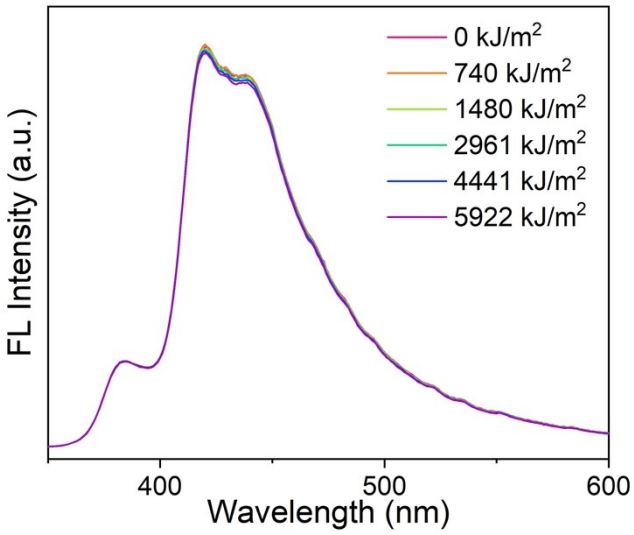

Fig. S5 UV dose-dependent luminescence spectra of bppCOOH under 365 nm UV excitation.

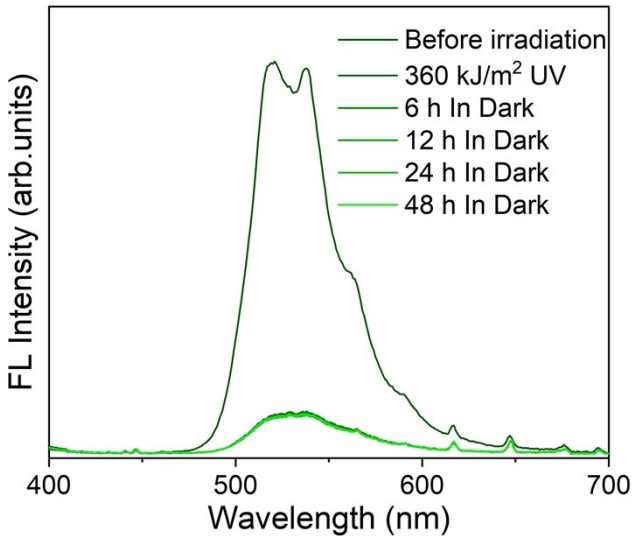

Fig. S6 Photoluminescence spectra of **U-bppCOO** before UV irradiations, after UV irradiations, and after being stored in dark.

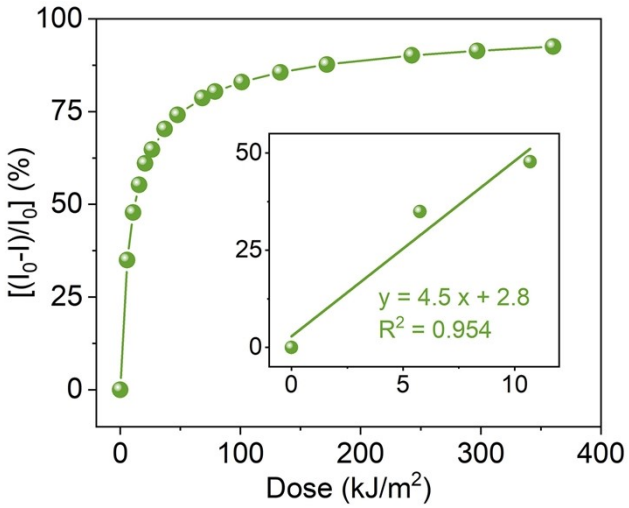

Fig. S7 The luminescence quenching rate of **U-bppCOO** as a function of UV dose. Inset: the quenching rate as a function of UV dose at the low dose range.

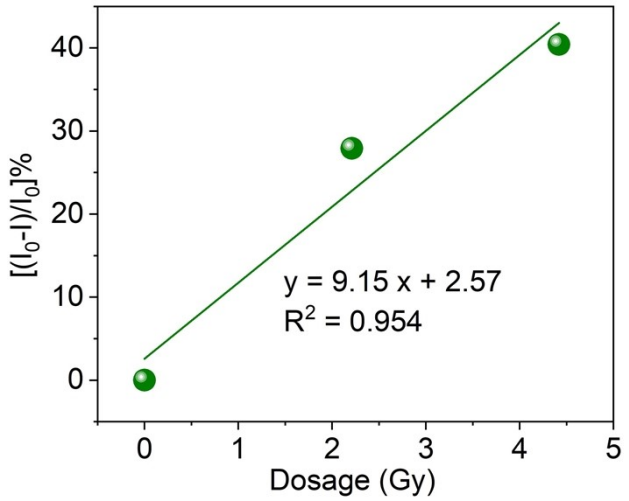

Fig. S8 The luminescence quenching rate of **U-bppCOO** as a function of X-ray dose at the low dose range.

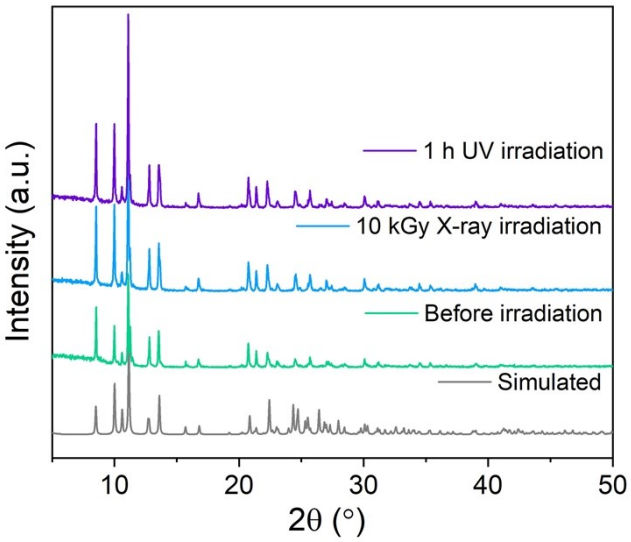

Fig. S9 Powder X-ray diffraction patterns of nonirradiated and irradiated **U-bppCOO**.

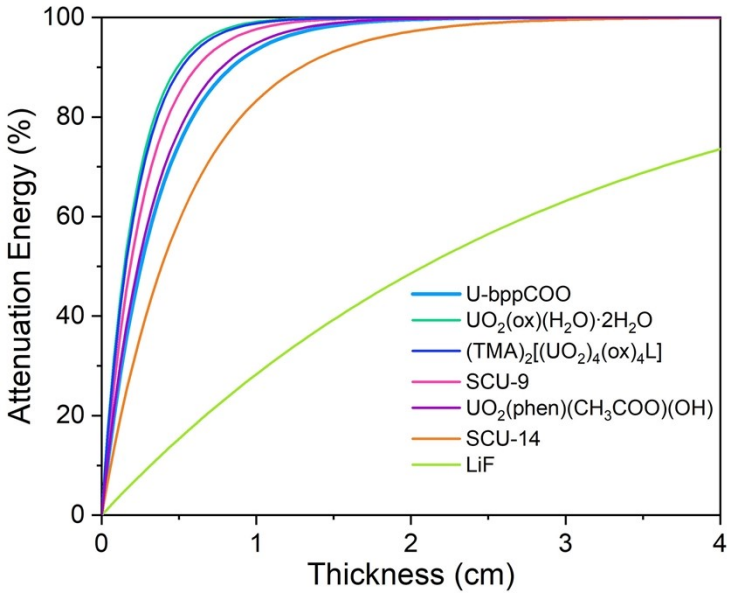

Fig. S10 X-ray attenuation efficiencies as the function of materials thickness of **U-bppCOO**, other uranium-based materials, or dosimeters (X-ray photon energy is 150 keV). Attenuation efficiency T is defined as $T = 1 - e^{-\mu_L x}$, where μ_L is the linear attenuation coefficient as defined by $\rho\mu_m$, x is the effective retarding thickness, ρ is the density, and μ_m is the mass attenuation coefficient. μ_m can be obtained from the photon cross sections database XCOM (https://physics.nist.gov/PhysRefData/Xcom/html/xcom1.html).

S4. Supplementary Tables.

Table S1 Crystallographic data for **U-bppCOO**.

Compound	**U-bppCOO**
Mass	572.82
Colour and habit	Yellow, acicular
Space group	$P2_1/c$
a (Å)	20.813(2)
b (Å)	4.3839(3)
c (Å)	17.693(2)
α (°)	90
β (°)	93.952(10)
γ (°)	90
V (Å^3)	1610.5(3)
Z	4
T (K)	298(2)
λ (Å)	0.71073
Max 2θ (°)	49.996
ρ_{calcd} (g cm^{-3})	2.362
μ (Mo Ka)	0.71073
GOF	1.118
R_{int}	0.0829
R_1	0.0605
wR_2	0.1578

Table S2 Selected bond lengths of **U-bppCOO**.

Bond	Distance (Å)
U(1)-O(3)	1.832(17)
U(1)-O(4)	1.833(15)
U(1)-O(2)	2.412(15)
U(1)-O(1)#3	2.445(12)
U(1)-O(5)#2	2.442(15)
U(1)-O(5)	2.301(16)
U(1)-O(5)#1	2.536(15)
U(1A)-O(3A)	1.802(18)
U(1A)-O(4A)	1.789(17)
U(1A)-O(1A)#3	2.53(3)
U(1A)-O(2A)	2.34(3)
U(1A)-O(5A)	2.46(2)
U(1A)-O(5A)#1	2.46(2)
U(1A)-O(5A)#2	2.645(19)

Table S3 Comparison of LODs toward UV and X-ray between **U-bppCOO** and other uranyl bearing materials.

	UV	X-ray	Ref.
U-bppCOO	3.06 J/m^2 equivalent to 3.26×10^{-8} J	0.012 Gy	This work
$UO_2(phen)(CH_3COO)(OH)$	4.30×10^{-6} J	0.32 Gy	3

UO_2(5-NIPA)(DMF)	2.4×10^{-7} J	N/A	4
$[Hphen]_2[(UO_2)_2(ox)_3]$	6.9×10^{-9} J	N/A	5
$(TMA)_2[(UO_2)_4(ox)_4L]$	N/A	5.2×10^{-4} Gy	6
U-Cbdcp	N/A	0.093 Gy	7
$UO_2(ox)(H_2O)\cdot 2H_2O$	N/A	1.18×10^{-5} Gy	8

Reference.

1. *Bruker APEX3 Software Suite; Bruker AXS Inc.: Madison, WI, 2016*.
2. G. M. Sheldrick, *Acta Crystallogr. Sect. C: Struct. Chem.*, 2015, **71**, 3.
3. H. Lu, Z. Zheng, J. Qiu, Y. Qian, J.-Q. Wang and J. Lin, *Dalton Trans.*, 2022, **51**, 3041.
4. W. Liu, X. Dai, J. Xie, M. A. Silver, D. Zhang, Y. Wang, Y. Cai, J. Diwu, J. Wang, R. Zhou, Z. Chai and S. Wang, *ACS Appl. Mater. Interfaces*, 2018, **10**, 4844.
5. J. Xie, Y. Wang, D. Zhang, C. Liang, W. Liu, Y. Chong, X. Yin, Y. Zhang, D. Gui, L. Chen, W. Tong, Z. Liu, J. Diwu, Z. Chai and S. Wang, *Chem. Commun.*, 2019, **55**, 11715.
6. J. Xie, Y. Wang, W. Liu, X. Yin, L. Chen, Y. Zou, J. Diwu, Z. Chai, T. E. Albrecht-Schmitt, G. Liu and S. Wang, *Angew. Chem. Int. Ed.*, 2017, **56**, 7500.
7. Z. Zheng, J. Qiu, H. Lu, J.-Q. Wang and J. Lin, *RSC Adv.*, 2022, **12**, 12878.
8. J. Xie, Y. Wang, W. Liu, C. Liang, Y. Zhang, L. Chen, D. Sheng, Z. Chai and S. Wang, *Sci. China Chem.*, 2020, **63**, 1608.